Product Prediction: Intermediates Formed During Rare Earth Reactions

Rodrigo Castañeda,*[1,2] Elizabeth Chavira,[1] and Oscar Peralta[2]

[1] Instituto de Investigaciones en Materiales, Universidad Nacional Autónoma de México, 04510 México DF, México.
   rodrigorho@yahoo.com; chavira@iim.unam.mx
[2] Centro de Ciencias de la Atmósfera, Universidad Nacional Autónoma de México, 04510 México DF, México. E-mail:
   oscar@atmosfera.unam.mx

Abstract. Thermal analyses, X-ray diffraction (XRD), and HR-XRD (High Resolution XRD) were used to identify thermal behavior products in a family of solid-state reactions involving rare earth (REE) reagents. REE where sorted in light and heavy groups. The general reactions under study were: $REE_2O_3 + Fe_2O_3 + As_2O_3 \rightarrow 2REEFeO_3 + As_2O_3\uparrow$ and $2REE(OH)_3 + Fe_2O_3 + As_2O_3 \rightarrow 2REEFeO_3 + As_2O_3\uparrow + 3H_2O\uparrow$, REE= La, Ce, Nd, Sm, Gd, Dy, Ho, Er, and Yb. Based on the experimental results, it is possible to predict the different compounds of REE products in a series of reactions analyzing only three of the reactions, two for light REE and one for heavy REE.
Key words: Rare-earth, XRD, TG-DSC, solid-state reaction, thermal stability

Resumen. Se realizaron análisis térmicos, difracción de rayos X (DRX) y DRX-AR (DRX de Alta Resolución) para identificar el comportamiento térmico de los productos de reacciones en estado sólido con tierras raras. Las tierras raras se agruparon en ligeras y pesadas. Las reacciones que se estudiaron fueron: $REE_2O_3 + Fe_2O_3 + As_2O_3 \rightarrow 2REEFeO_3 + As_2O_3\uparrow$ y $2REE(OH)_3 + Fe_2O_3 + As_2O_3 \rightarrow 2REEFeO_3 + As_2O_3\uparrow + 3H_2O\uparrow$, REE= La, Ce, Nd, Sm, Gd, Dy, Ho, Er, y Yb. Basándonos en los resultados de este procedimiento experimental, se pueden predecir los diferentes compuestos en una familia de reacciones analizando solo tres de las reacciones, dos para los REE ligeros y una para los REE pesados.
Palabras clave: Tierra rara, DRX, TG-DSC, reacción en estado sólido, estabilidad térmica.

Introduction

Rare earth orthoferrites, $REEFeO_3$ present interesting properties when iron is substituted [1, 2] with another transition metal. For example, a partial Fe substitution with Mn in the yttrium orthoferrite, $YFe_{1-x}Mn_xO_3$, changes its magnetic behavior dramatically [1]. The substitution induces a spin-reorientation transition from the low-temperature antiferromagnetic state to a high-temperature weak ferromagnetic state. As far as we know, there are no studies around the substitution of arsenic in rare earth orthoferrites. Trivalent arsenic (As^{3+}), in an octahedral site, is the same size as Mn^{3+}, roughly 72 pm. It is interesting to research that cation substitution.

There is a lack of literature on the formation of rare earth orthoferrites. One of the few available reference found was that of Parida. Parida *et al.* [3] studied the thermodynamic properties of $LaFeO_3$ and determined its enthalpy increments and standard molar Gibbs energy of formation; but the thermal stability and reactions expected phases that precede the main product remain unknown.

On our study, rare earth elements were separated into two groups sorted by molecular weight using the classification by Barret and Dhesi [4]: a) light rare earth, from lanthanum to samarium, and b) heavy rare earth, from gadolinium to lutetium. Within each group, the chemical properties of the elements are very similar. The advantage of studying the REE as light and heavy is that the chemical behavior of each group is expected to be the same. The reactions selected were $REE_2O_3 + Fe_2O_3 + As_2O_3 \rightarrow 2REEFeO_3 + As_2O_3\uparrow$ and $2REE(OH)_3 + Fe_2O_3 + As_2O_3 \rightarrow 2REEFeO_3 + As_2O_3\uparrow + 3H_2O\uparrow$. The reagents used were: La_2O_3, $La(OH)_3$, Gd_2O_3, CeO_2, Pr_6O_{11}, and the corresponding oxides of Nd, Sm, Dy, Ho, Er, and Yb (REE_2O_3).

Only La_2O_3, $La(OH)_3$, and Gd_2O_3 were treated to guarantee their chemical form, all the other rare earth reagents were used as were stored, some of the reagents were in hydroxide form.

Thermal analyses (thermogravimetric analysis, TG, and differential scanning calorimetry, DSC) were used to determine the thermal stability of the compounds and temperatures at which thermal events occur. To understand the reactions process, three reactions, that are representative of the light and heavy REE groups, were fully studied to determine the intermediate products at selected temperatures; two with light REE, $La_2O_3 + As_2O_3 + Fe_2O_3$, and $La(OH)_3 + As_2O_3 + Fe_2O_3$, and one with a heavy REE, $Gd_2O_3 + As_2O_3 + Fe_2O_3$. Light REE oxides can absorb water easily and transform to hydroxides, which is why the analysis contemplate both forms. Temperatures between thermal events were chosen for each of the three reactions to determine their behavior at each temperature. Using the first derivative of the DSC (Fig. 1 and 2) the thermal events between 25 to 700 °C can be determine, in the middle of two thermal events a temperature was chosen. At the selected temperatures, a sample of reactants was heated and then cooled gradually (C) inside the furnace and quenched in ice (Q) in a platinum pan. Cooling gradually allows the reactions to form stable compounds. Quenching in ice permits the identification of metastable compounds. X-ray diffraction (XRD) was used to identify reagents, products, and intermediate products between thermal events for the reactions with La_2O_3 and Gd_2O_3, while HR-XRD (High Resolution X-Ray Diffraction) was performed for the $La(OH)_3$ reaction. The use of HR-XRD allowed to identify the intermediate products clearly.

The reactions $REE_2O_3 + Fe_2O_3 + As_2O_3 \rightarrow 2REEFeO_3 + As_2O_3\uparrow$ and $2REE(OH)_3 + Fe_2O_3 + As_2O_3 \rightarrow 2REEFeO_3 + As_2O_3\uparrow + 3H_2O\uparrow$ were selected to study the substitution of arsenic in the
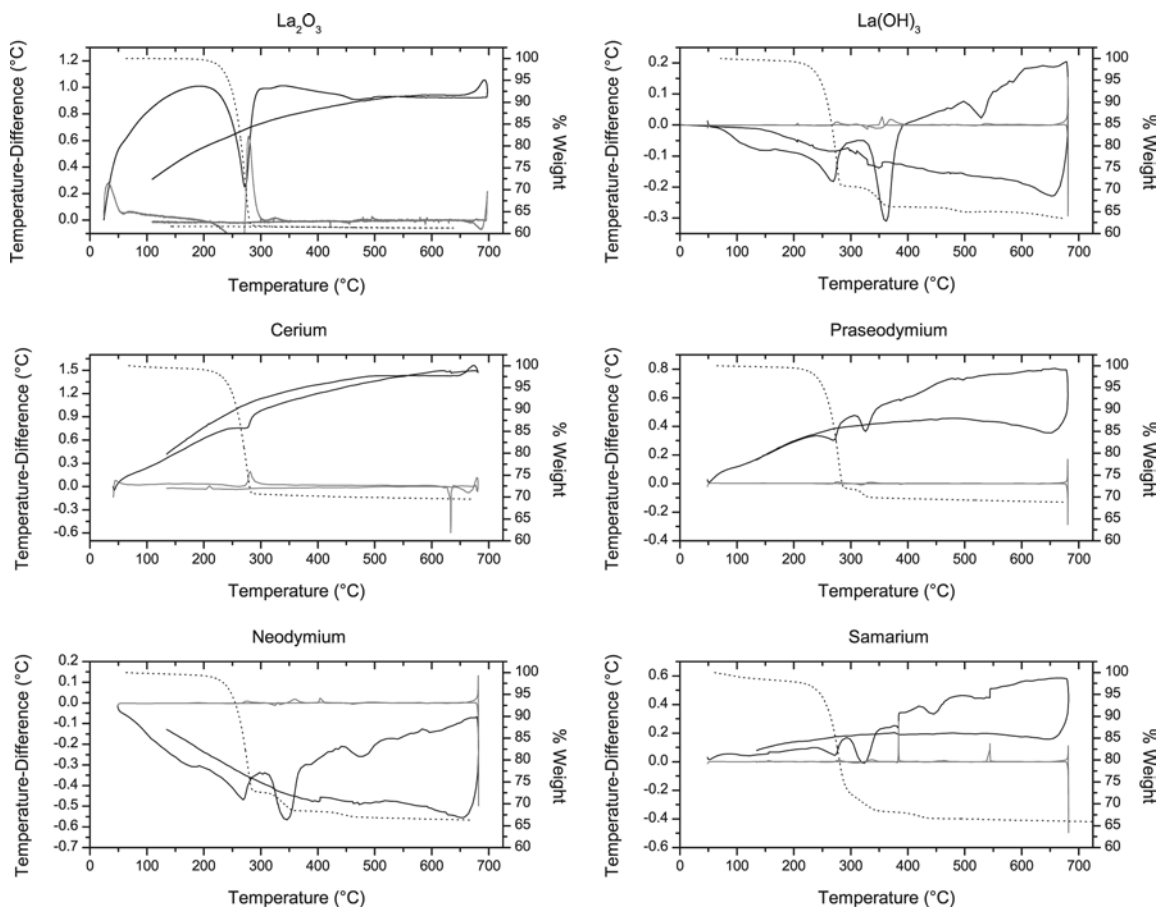
Fig. 1. TG and DSC analyses for La_2O_3, $La(OH)_3$, Ce, Pr, Nd, and Sm reactions. TG (dotted line), DSC (solid black), and DSC first derivative (solid gray).

iron site of orthoferrites. The thermal characterization was necessary to understand step by step the reaction process. After analyzing the TG and DSC curves it was decided to do the identification of phases between thermal events because of the similarities in the thermal (TG and DSC) behavior of all the reactions.

Results and Discussion

The investigation consisted of two main procedures: the thermal characterization of the reactions and the identification of phases in the reactions. For the thermal characterization of the reactions, TG and DSC were selected. The thermal analyses for each of the eleven reactions between 25 and 700 °C were done. The second procedure consisted of the identification of phases formed at different temperatures in a range from 25 to 700 °C for the reactions with La_2O_3, $La(OH)_3$, and Gd_2O_3 using two cooling methods; gradually cooled (C) in air until ambient temperature was reached and quenched in ice (Q) at about 1 °C.

Thermal characterization

TG and DSC analyses are compared in Figs. 1 and 2, TG (dotted line), DSC (solid black) and the first derivative of DSC

(solid gray). There was weight loss between 28% for the reaction with Er, and 37% for $La(OH)_3$. The weight loss took place with two distinct patterns. The first pattern had one slope, for the reactions with La_2O_3, Ce, Gd_2O_3, Dy, Ho, Er, and Yb, that started approximately at 190 °C and ended around 270 °C. The second pattern had two slopes for reactions with $La(OH)_3$, Pr, Nd, and Sm; the first slope behaved similarly to the one in the first pattern with same start and end temperatures. The second slope started approximately at 270 °C and ended at 350 °C. There was a clear relation between the reactions with the same behavior.

Neumann *et al.* [5] studied the decomposition of pure $La(OH)_3$ where TG presented two slopes, similar to the present case. They found for pure $La(OH)_3$ that the total weight loss was 15% and the first slope started at 320 °C and ended at 400 °C. The second slope started at 400 °C and ended at 550 °C. The reported reactions for the decomposition of pure $La(OH)_3$ are: $2La(OH)_3 \rightarrow 2LaOOH + 2H_2O\uparrow \rightarrow La_2O_3 + H_2O\uparrow$. The decomposition of pure $La(OH)_3$ shed light in the possible intermediates that could be found. In the case of our reaction, $2La(OH)_3 + Fe_2O_3 + As_2O_3 \rightarrow 2REEFeO_3 + As_2O_3\uparrow + 3H_2O\uparrow$, the weight loss was 37% and the first slope started at 190 °C. There is a shift in temperature, comparing the decomposition of pure $La(OH)_3$ with our reaction with $La(OH)_3$, caused by the
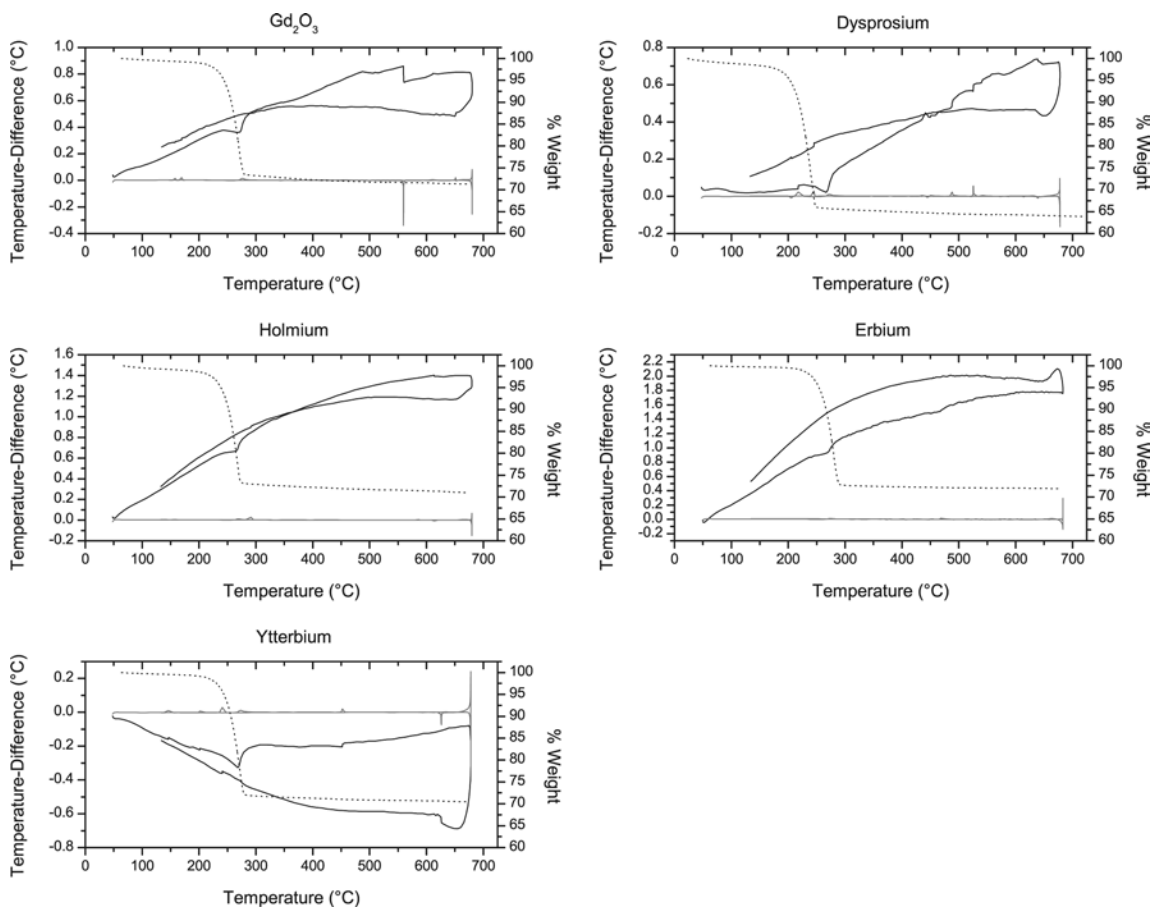
Fig. 2. TG and DSC analysis for Gd$_2$O$_3$, Dy, Ho, Er and Yb reactions. TG (dotted line), DSC (solid black), and DSC first derivative (solid gray).

mixture of compounds and the presence of As$_2$O$_3$. The weight loss posed a more sophisticated process to explain.

Weight loss cannot be superficial water; all reagents were dried at 120 °C for 24 h prior synthesis. A theoretical analysis of the maximum amount of water that these reactions could lose if the REE reagent was RE(OH)$_3$ was done. The loss weight due to water would be between 12% for reaction with yttrium hydroxide and 14% for reaction with lanthanum hydroxide. Table 1 portrays the theoretical weight loss of the reactions assuming all rare earth reagents were in their hydroxide form. Other factors for the loss weight are the reagents in question: Fe$_2$O$_3$ has a melting point of 1565 °C [6], while REE oxides have a melting point between 2230 °C for Ce$_2$O$_3$ to 2435 °C

for Yb$_2$O$_3$ [7]. The melting points of As$_2$O$_3$ polymorphs are 272 – 315 °C for arsenolite [8, 9, 10, and 11], 193 – 314 °C [9, 10, and 12] for claudetite, and the boiling point for both compounds are 460 °C [9]. The weight loss was because the As$_2$O$_3$, which represented between 26% for the reaction with Yb$_2$O$_3$ and 36% for the reaction with La(OH)$_3$, evaporated. The evaporation of arsenic oxide was complete, the weight loss was higher for every reaction that the As$_2$O$_3$ could be accounted for.

The reactions with La$_2$O$_3$, Ce, Gd$_2$O$_3$, Dy, Ho, Er, and Yb had two principal thermal events, while for the reactions with La(OH)$_3$, Pr, Nd, and Sm there are three main thermal events. Comparing the thermal analyses (TG and DSC) of light REE with La$_2$O$_3$ and La(OH)$_3$, indicated that each different com-

Table 1. Maximum theoretical weight loss in the reactions if all the rare earthreagentswere in hydroxide form and the experimental weight loss presented in the reactions.

Compound	Theo. weightloss (%)	Exp. weightloss (%)	Compound	Theo. weightloss (%)	Exp. weightloss (%)
La(OH)$_3$	14.2	39	Gd(OH)$_3$	13.0	29
Ce(OH)$_3$	14.1	31	Dy(OH)$_3$	12.6	36
Pr(OH)$_3$	14.1	31	Ho(OH)$_3$	12.5	29
Nd(OH)$_3$	13.8	34	Er(OH)$_3$	12.4	28
Sm(OH)$_3$	13.4	34	Yb(OH)$_3$	12.0	30

Table 2. Compounds present at different temperatures cooled with two methods, gradually (C) and by quenching (Q), for La_2O_3, $La(OH)_3$, and Gd_2O_3 reactions.

La_2O_3		$La(OH)_3$		Gd_2O_3	
Gradual	*Quench*	*Gradual*	*Quench*	*Gradual*	*Quench*
175°C		200°C		150°C	
La_2O_3, As_2O_3, α-Fe_2O_3		$La(OH)_3$, As_2O_3, α-Fe_2O_3		Gd_2O_3, As_2O_3, α-Fe_2O_3	
308 °C		310 °C		345 °C	
La_2O_3, α-Fe_2O_3	La_2O_3, **As_2O_3**, α-Fe_2O_3	$La(OH)_3$, α-Fe_2O_3, LaOOH	$La(OH)_3$, α-Fe_2O_3, LaOOH	Gd_2O_3, α-Fe_2O_3	
380 °C		440 °C		510 °C	
La_2O_3, α-Fe_2O_3		α-Fe_2O_3, LaOOH, $Fe_3(AsO_4)\cdot2(H_2O)_8$	α-Fe_2O_3, LaOOH,**La_2O_3** $Fe_3(AsO_4)\cdot2(H_2O)_8$	Gd_2O_3, α-Fe_2O_3	
575 °C		600 °C		590, 630 and 666 °C	
La_2O_3, α-Fe_2O_3		α-Fe_2O_3, $La(OH)_3$, LaOOH	α-Fe_2O_3, $La(OH)_3$, LaOOH	Gd_2O_3, α-Fe_2O_3	

Metastable phases in **bold** and stable phases in plain font.

pound found for these reactions ought to be the same for all other light REE reactions, and all the compounds found in the Gd_2O_3 reaction must be the same for the heavy REE reactions. The temperature of the formation of each compound changes from reaction to reaction, but that temperature can be obtained using the DSC analysis.

The final product $LnFeO_3$ (Ln = La, Ce, Pr, Nd, Sm, Gd, Dy, Ho, Er and Yb) was analyzed by XRD, indicating that all structures were orthorhombic with a space group P*nma*, No. 62. As the compositions were isostructural, the changes of the compounds found should be similar in light and in heavy REE reactions.

Identification of phases

The reactions with $La(OH)_3$, La_2O_3 and Gd_2O_3 were further studied to found the compounds synthesized for each reaction between thermal events. A set of temperatures were selected for each of these three reactions between thermal events. The following temperatures were chosen for La_2O_3 (175, 308, 380, and 575 °C); for $La(OH)_3$ (200, 310, 440, and 600 °C), and for Gd_2O_3 (150, 345, 510, 590, 630, and 666 °C) in order to study the phases present in the reactions. The temperatures were selected using the first derivative of the DSC; the first step was identifying the pikes, temperatures at which a thermal event occurs, and the second step was selecting a temperature between two pikes, between thermal events.

About 0.2 g of each reactive reagents were heated at every temperature and then cooled by two methods, gradually cooling (C) and quenching in ice (Q). The cooled samples were studied by XRD, for La_2O_3 and Gd_2O_3 reaction, and by HRXRD, for the reaction with $La(OH)_3$, at room temperature. All the phases found by Q and C for the La_2O_3, $La(OH)_3$, and Gd_2O_3 reactions are shown in Table 2. Also, the nine HR-XRD diffractograms for $La(OH)_3$ reaction are presented in Fig. 3, the main peaks for each of the six phases found are labeled.

The reaction with La_2O_3 and Gd_2O_3 showed, as was presented earlier, the evaporation of arsenic oxide, As_2O_3, as the principal thermal event. Only three compounds were found in those reactions in the whole range of temperature. In the $La(OH)_3$ reaction, however, six different compounds were found between 25-700 °C. The addition of OH⁻ radicals, with $La(OH)_3$, changed the reaction because those groups tend to easily react with the surrounding atoms. We deduce that the hydroxyl group was capable of stabilizing the arsenide oxide; while with La_2O_3 and Gd_2O_3 the arsenic oxide evaporated, in the reaction with $La(OH)_3$, As_2O_3 reacted and formed parasymplesite ($Fe_3(AsO_4)_2\cdot8(H_2O)$).

The state of the reagent's rare earth compound, REE_2O_3 or $REE(OH)_3$ REE= La, Ce, Nd, Sm, Gd, Dy, Ho, Er, and Yb, for the other eight reactions, can be identified comparing the TG curves (Figs. 1 and 2) to the thermal analyses of La_2O_3, $La(OH)_3$, and Gd_2O_3 reactions. The following compounds were in oxide form, REE_2O_3: cerium, dysprosium, holmium, erbium, and ytterbium. These compounds were found to have lost weight in one stage, as in La_2O_3 and Gd_2O_3 reactions. The hydroxides, $REE(OH)_3$ were praseodymium, neodymium, and samarium. All these compounds had a two-stage weight loss, as in the reaction with $La(OH)_3$.

Knowing the conditions at which a compound is going to be synthesized could be of great service to other researchers. For example, Hosono *et al.* [13] aimed at obtaining a superconductor thin film using a pulsed laser deposition technique. The temperature of the substrate was set to 600 and 800 °C, at these temperatures their search was for nought, had the present paper been available, it would have shed light into the fact that at 600 and 800 °C the stable products are a mixture of compounds (La_2O_3, LaOF, LaAs, $LaFeO_3$, FeAs and Fe_2As) [13], and that the product they looked for was hardly going to be synthesized under such conditions.

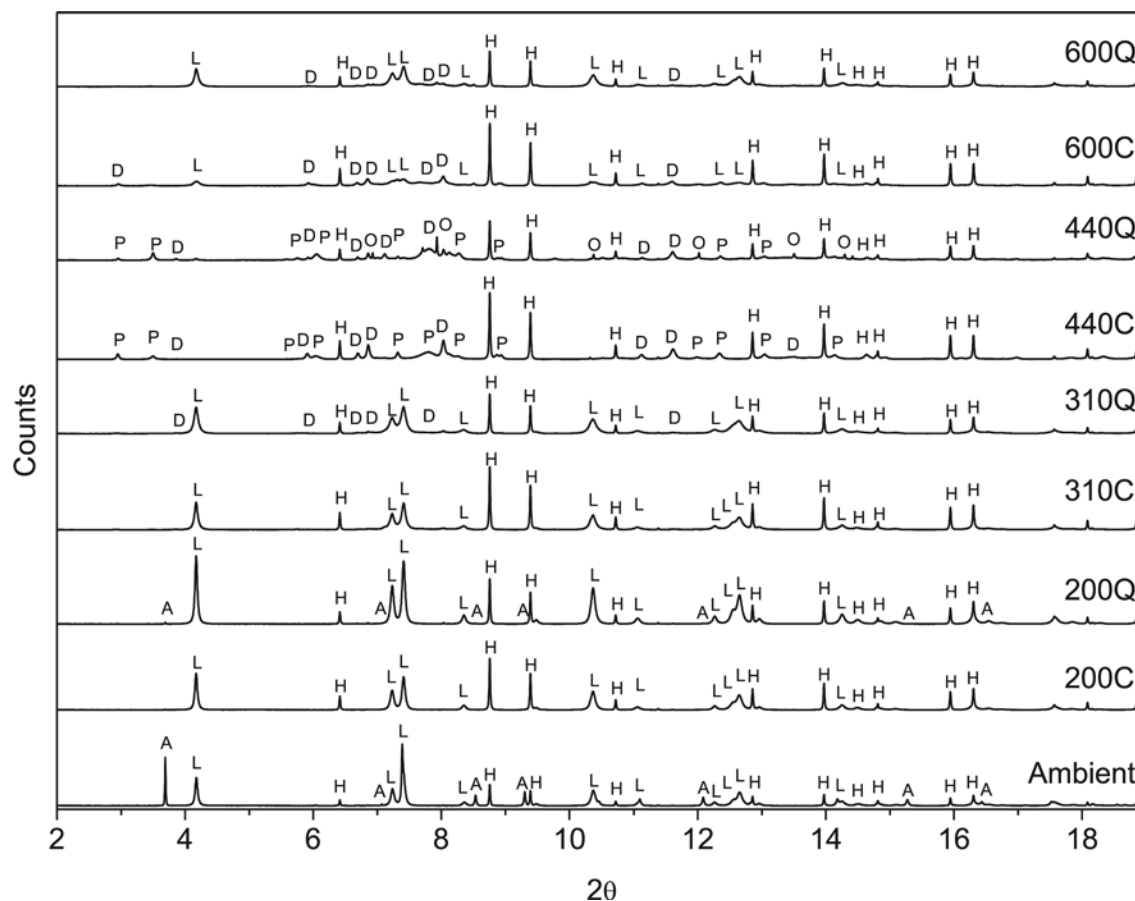**Fig. 3.** HR-XRD for the La(OH)$_3$ reaction at the selected temperatures using the two cooling methods, Q and C. The letters correspond to H: Fe$_2$O$_3$ (PDF 00-033-0664), L: La(OH)$_3$ (PDF 00-036-1481), A: As$_2$O$_3$ (00-036-1490), D: LaOOH (PDF 00-013-0436), P: Fe$_3$(AsO$_4$)$_2$·8(H$_2$O) (PDF 01-075-1187), and O: La$_2$O$_3$ (PDF 00-005-0602).

To conclude, the system of implementation put forward here is simple and can be used to predict what compounds can be expected with different reagents in the same family, especially in rare earth reactions, at different temperatures between thermal events. The mixture of compounds and phases can be obtained using the same reaction path, stoichiometry, and heat temperature associated to a TG and DSC analysis. The reactions REE$_2$O$_3$ + Fe$_2$O$_3$ + As$_2$O$_3$ → 2REEFeO$_3$ + As$_2$O$_3$↑ are straight forward when the rare earth reagent is in oxide form, the main event is the evaporation of arsenic oxide. When the reagent is in hydroxide form, 2REE(OH)$_3$ + Fe$_2$O$_3$ + As$_2$O$_3$ → 2REEFeO$_3$ + As$_2$O$_3$↑ + 3H$_2$O↑, the reaction is complex. Six products were found in the La(OH)$_3$ reaction, including para-symplesite. It is important to predict what phases are going to be formed in a series of reactions, rare earth reactions in this case, to optimize time and resources.

Experimental

The thermal characterization of the reactions, REE$_2$O$_3$ + Fe$_2$O$_3$ + As$_2$O$_3$ → 2REEFeO$_3$ + As$_2$O$_3$↑ and 2REE(OH)$_3$ + Fe$_2$O$_3$ + As$_2$O$_3$ → 2REEFeO$_3$ + As$_2$O$_3$↑ + 3H$_2$O↑ REE= La, Ce,

Nd, Sm, Gd, Dy, Ho, Er, and Yb, was done by TG and DSC (Figs. 1 and 2). Reagents, except La$_2$O$_3$, La(OH)$_3$, and Gd$_2$O$_3$, were used without modification to their storage conditions. To ensure the presence of lanthanum oxide and gadolinium oxide, the compounds were dehydrated in a furnace at 1000 °C for 12 h in air and corroborated by XRD. Superficial water was eliminated heating all the reagents at 120 °C for 24 h in air. REE, Fe$_2$O$_3$, and As$_2$O$_3$ poly-crystals (purities above 99.9%) were mixed in an agate mortar and pestle until the mixture became homogeneous. The main product was identified using XRD (not presented in this paper).

The second procedure consisted on the identification of phases formed from 25 °C to 700 °C for the following reactions: a) La(OH)$_3$ + Fe$_2$O$_3$ + As$_2$O$_3$, b) La$_2$O$_3$ + Fe$_2$O$_3$ + As$_2$O$_3$, and c) Gd$_2$O$_3$ + Fe$_2$O$_3$ + As$_2$O$_3$. To identify the changes in phases, the DSC was examined to determine temperatures between thermal events. A mixture of the reagents, about 0.2 g, was heated at these temperatures for 20 minutes in a platinum pan and then cooled down by two methods: i) by quenching (Q) in ice and ii) by gradually cooling (C) in air inside the furnace. These procedures allowed the identification of stable and metastable phases. Cooling by quenching allowed us to identify metastable phases because that phase gets trapped at
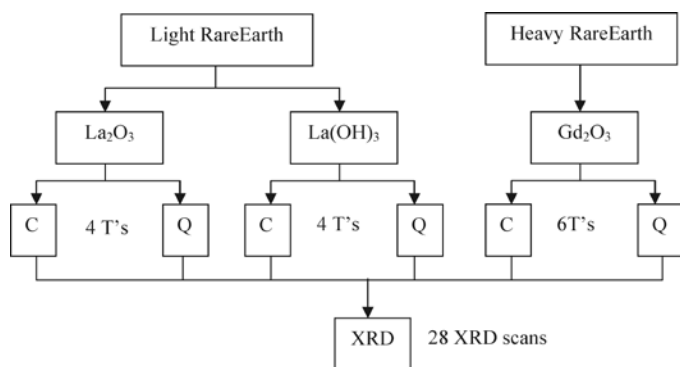
that temperature, gradually cooling allows the phase to rearrange and return to a stable phase. The resulting phases were characterized using XRD for the reactions with La_2O_3 and Gd_2O_3 and HR-XRD for the $La(OH)_3$ reaction, Fig. 3 shows the HR-XRD for the reaction with lanthanum hydroxide. Scheme 1 illustrates the process.

Characterization techniques

TG and DSC measurements were performed in a TA Instruments SDT Q600 at 10 °C min^{-1} and 60 mL min^{-1} flow rate of air with sample weight between 3.5 and 3.9 mg in alumina open crucible. The thermal program was 25-700-25 °C.

The samples were characterized at room temperature in air by XRD on a Bruker D-8 diffractometer coupled to a copper X-ray anode tube and a graphite diffracted beam monochromator (Cu-K$_\alpha$; $\lambda = 1.54$ Å). The diffractograms were measured from 10° to 75° (2θ) with a 0.016° (2θ) step scanning.

For the reactions with $La(OH)_3$, HR-XRD was used. The measurement was done at Argone National Laboratory in Beamline 11-BM. The wavelength used was 0.412239 Å and the scan was measured from 0 to 30 °2θ with a step size of 0.003 °2θ. The photon source is obtained with a bending magnet (BM) with a critical energy of 19.5 keV that delivers around 5×10^{11} phs/s @ 30 keV, and a monochromator of Si(111).

Detection was done with 12 independent analyzers with a 2 °2θ separation. The analyzer consisted on Si(111) crystals and $LaCl_3$ scintillation detectors.

Scheme 1. Flux diagram for the identification of phases. Two branches, one for light REE (La_2O_3 and $La(OH)_3$) and the other for heavy REE (Gd_2O_3).

References

1. Sundarayya, Y.; Mandal, P.; A. Sundaresan; C.N.R. Rao. *Phys. Condens. Matter*. **2011**, *23*, 436001.
2. Acharya, S.; Chakrabarti, P.K. *Solid State Commun*. **2010**, *150*, 1234-1237.
3. Parida, S. C.; Singh, Z.; Dash, S., Prasal, R.; Venugopal, V. *J. All. Comp*. **1998**, *280*, 94-98.
4. Cotton, S.E.; Dhesi, S.S. *The structure of rare-earth metal surfaces*, London Imperial College, **2001.**
5. Neumann, A.; Walter, D. *Thermochim. Acta*. **2006**, *445,* 200-204.
6. Cotton, F. A.; Wilkinson, G.; Murillo, C.A.; Bochmann, M. *Advanced Inorganic Chemistry*, John Wiley & Sons, **1999.**
7. Dean, J.A. *Lange's Handbook of Chemistry*, 5th edition, McGraw-Hill, Inc., **1999.**
8. Knacke, I.; Barin, O. *Thermochemical properties of inorganic substances*, 15th edition, Springer, **1973.**
9. Barin, A. *Thermochemical Data of Pure Substances*, VCH Verlags-Gesellschaft GmbH, Weinheim, **1989.**
10. Wells, F. *Structural Inorganic Chemistry*, 5th edition, Clarendon press, Oxford, **1984.**
11. Rushton, E. R.; Daniels, F. *J. Am. Chem. Soc*. **1926**, 48, 384.
12. Weast, R.C. *CRC Handbook of Chemistry and Physics*, The Chemical Rubber Co., Ohio, **1970.**
13. Hiramatsu, H.; Kamiya, T.; Hirano, M.; Hosono, H. *Physica C.* **2009**, 469, 657-666.